Indonesian Journal of Science & Technology

Journal homepage: http://ejournal.upi.edu/index.php/ijost/

Computational Engineering of Malonate and Tetrazole Derivatives Targeting SARS-CoV-2 Main Protease: Pharmacokinetics, Docking, and Molecular Dynamics Insights to Support the Sustainable Development Goals (SDGs), with a Bibliometric Analysis

Mohammed Merzouki[1], Oussama Khibech[1], Elmehdi Fraj[1], Haytham Bouammali[1], Chaymae Bourhou[1], Belkheir Hammouti[2,], Boufelja Bouammali[1], Allal Challioui[1]*

[1]University Mohamed Premier, Oujda, Morocco
[2]Euromed University of Fes, Morocco
[*]Correspondence: E-mail: hammoutib@gmail.com

ABSTRACT

This research applies computational engineering to explore malonate and tetrazole derivatives as potential inhibitors of the SARS-CoV-2 Main Protease. A comprehensive in silico approach, including pharmacokinetics prediction, molecular docking, and molecular dynamics simulations, was utilized to evaluate the drug-likeness, binding affinity, and stability of the designed compounds. The malonate derivatives demonstrated strong interaction stability with the target protease and exhibited favorable pharmacokinetic profiles with minimal predicted toxicity, supporting their potential as therapeutic candidates. A bibliometric analysis was also performed to position this study within the broader scientific landscape, showing increasing global interest in SARS-CoV-2 protease inhibitors and antiviral drug development. This work aligns with the Sustainable Development Goals by contributing to global health improvement and fostering innovation in pharmaceutical engineering. The promising computational outcomes underscore the need for further experimental validation to confirm therapeutic efficacy and safety, potentially contributing to future antiviral treatment strategies.

ARTICLE INFO

Article History:
Submitted/Received 25 Mar 2025
First Revised 29 Apr 2025
Accepted 02 Jun 2025
First Available Online 03 Jun 2025
Publication Date 01 Sep 2025

Keyword:
ADMET analysis,
Malonates,
Molecular docking,
Molecular dynamics simulation,
SARS-CoV-2 Mpro,
Tetrazoles.

1. INTRODUCTION

The global outbreak of coronavirus disease, caused by severe acute respiratory syndrome coronavirus 2 (SARS-CoV-2), has posed an unprecedented challenge to global health systems and stimulated extensive research efforts worldwide [1]. The COVID-19 pandemic has profoundly altered many aspects of human life, including healthcare systems, economic activities, educational processes, and daily social interactions, as evidenced by widespread shifts in medical priorities, global supply chains, remote learning, and public health policies, as reported elsewhere [2-16].

SARS-CoV-2 is a positive-sense single-stranded RNA virus belonging to the Coronaviridae family, sharing significant similarity with the earlier SARS-CoV [17]. The virus utilizes multiple proteins for its replication cycle, among which the main protease (Mpro) plays a crucial role in processing viral polyproteins essential for replication [18, 19]. Due to its essential function and absence in human host proteases, Mpro has been widely recognized as an attractive therapeutic target for antiviral drug development [20]. Many research regarding covid has been well-documented [21-25].

In response to this urgent need, various computational approaches have been adopted to accelerate the drug discovery process. In silico methods such as molecular docking, pharmacokinetics prediction, and molecular dynamics simulation offer efficient and cost-effective strategies to identify and optimize potential drug candidates before entering experimental stages [26, 27]. These computational frameworks enable early evaluation of pharmacological properties, toxicity profiles, and structural stability of candidate molecules, substantially reducing the risks and costs associated with laboratory trials [28].

In this study, novel malonate and tetrazole derivatives were systematically designed and evaluated through an integrated computational engineering workflow. The selection of malonate and tetrazole scaffolds was based on their structural diversity and promising bioactivity profiles reported in prior studies [29, 30]. Molecular docking and molecular dynamics simulations were employed to assess their binding interactions with the SARS-CoV-2 main protease. Pharmacokinetic and ADMET analyses were conducted to predict their absorption, distribution, metabolism, excretion, and toxicity profiles, ensuring their suitability for potential oral administration [31, 32]. Furthermore, a bibliometric analysis was incorporated to examine current scientific trends and research development related to SARS-CoV-2 main protease inhibitors. This analysis provides a broader perspective on the global scientific landscape and emphasizes the relevance of this research within ongoing drug discovery efforts [33, 34].

The novelty of this work lies in the combined application of advanced computational engineering, multi-dimensional pharmacokinetics analysis, molecular dynamics simulation, and bibliometric evaluation in designing malonate and tetrazole derivatives as promising SARS-CoV-2 Mpro inhibitors. In addition, this research highlights its contribution to the Sustainable Development Goals (SDGs) by advancing innovations in health-related technologies and global pandemic preparedness, as reported elsewhere [35-49]. These integrated approaches aim to support the early identification of potential antiviral agents that may contribute to future therapeutic strategies against COVID-19 and related viral infections.

DOI: https://doi.org/10.17509/ijost.v10i2.85146
p- ISSN 2528-1410 e- ISSN 2527-8045

2. METHODS

2.1. Ligand Preparations and Protein Preparations

In summary, all ligands of malonates 3a-3c and derivatives tetrazoles 4a-4c, along with the native ligand (N-[(5-METHYLISOXAZOL-3-YL)CARBONYL]ALANYL-L-VALYL-N1-((1R,2Z)-4-(BENZYLOXY)-4-OXO-1-{[(3R)-2-OXOPYRROLIDIN-3YL]METHYL}BUT-2-ENYL)-L-LEUCINAMIDE) obtained from PubChem (CID: 146025593) (**Figure 1**), were acquired in SDF format and imported into Maestro 12.8 (Schrödinger 2021-2) for ligand preparation in the docking process [29]. Ligand preparation serves not only to generate low-energy structures but also to extend each input structure to meet the required stereochemistry by producing tautomers and confirming changes in ring ionization states. To establish ionization states for each ligand structure at physiological pH (7±2 units), the Schrödinger Maestro's LigPrep wizard (Schrödinger 2021-2) was employed, utilizing Epic [30]. The ligands underwent minimization using the OPLS2005 force field, with other options left at their default settings. For subsequent docking with Glide, output files generated from the ligand minimization stage were utilized. The X-ray crystal structure of the COVID-19 main protease in complex with an inhibitor N3, with a crystalline structure resolution of 2.16 Å, was retrieved from the Protein Data Bank with PDB ID: 6LU7 (**Figure 2**) [31]. Chains A and B comprise the homodimeric Mpro. In this study, chain A was selected, prepared using Schrödinger's Protein Preparation Wizard, and utilized for the next-level investigation. Input data of the receptor was compiled by determining the receptor atoms, calculating the essential hydrogen atom's position, and defining and specifying the atoms of the binding site.

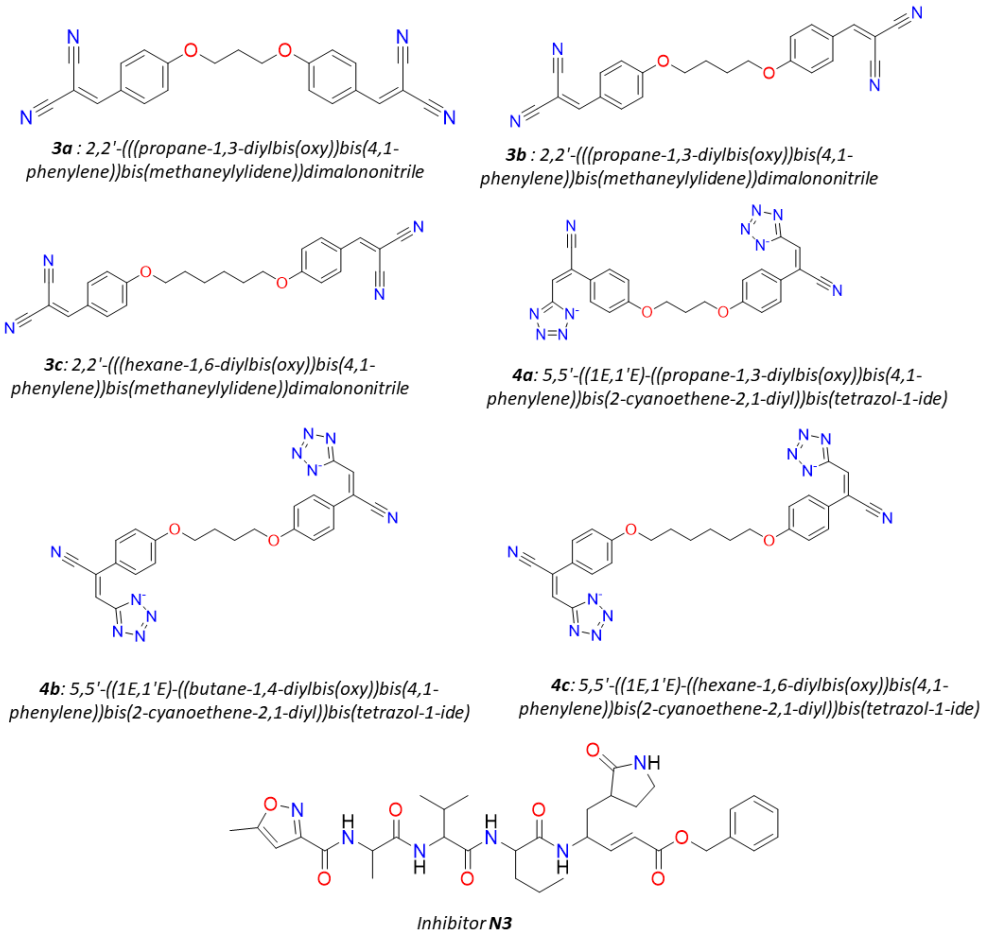

Figure 1. The 2D Structures of Compounds Used in the Current Study.

DOI: https://doi.org/10.17509/ijost.v10i2.85146
p- ISSN 2528-1410 e- ISSN 2527-8045

2.2. Pharmacokinetic Analysis using Computational Tools

A compound's pharmacokinetic profile, encompassing absorption, distribution, metabolism, and excretion (ADME), is shaped by an array of biochemical and physiological processes that dictate its behavior within biological systems [21]. A clear grasp of these factors is paramount to understanding how a compound is absorbed, carried throughout the body, metabolized, and eventually cleared. As computational technologies advance, in silico approaches are increasingly utilized to forecast ADME-related properties, enabling simulations of membrane permeability, biomolecular interactions during absorption and excretion, and overall structural integrity during metabolism. In this study, the initial step involved constructing the molecular structures of the investigated compounds using ChemDraw and converting them into SMILES format. These SMILES strings were then entered into SwissADME, pkCSM, and ADMETlab3 for in silico pharmacokinetic assessment [31]. Through robust predictive modeling, these platforms provided deeper insights into each compound's prospective pharmacological effectiveness and toxicity under conditions mirroring those of living organisms.

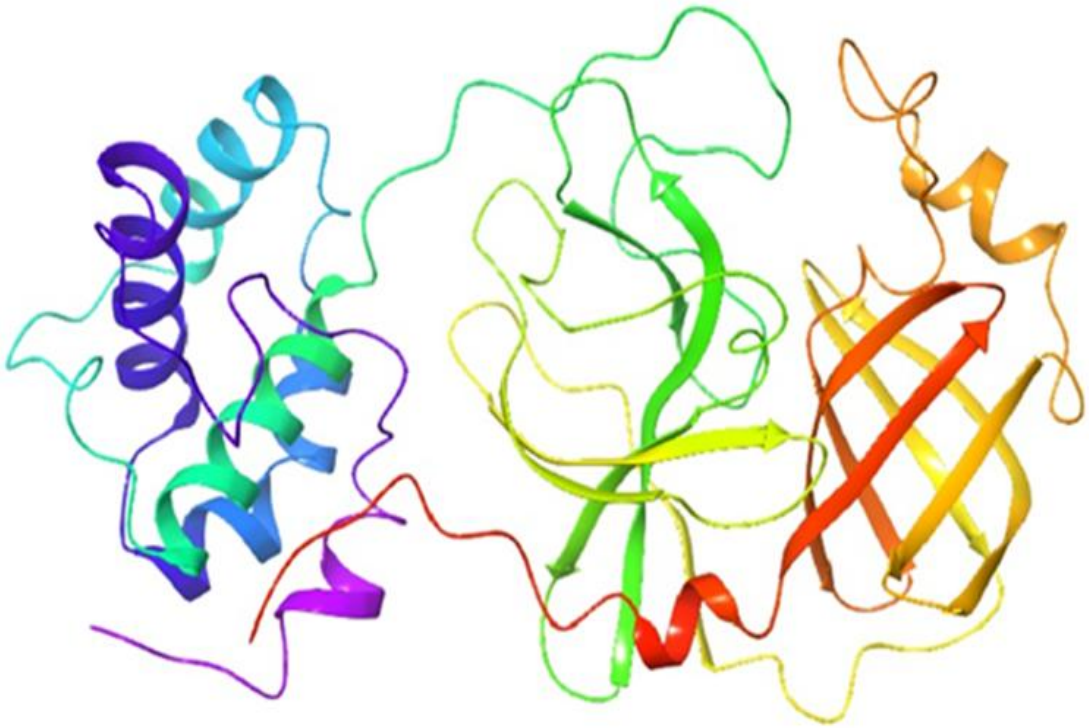

Figure 2. The crystal structure of SARS-CoV-2 Mpro (PDB ID: 6LU7).

2.3. Molecular Docking Calculations

For the docking process, the previously reduced and optimized protein was utilized. The initial step involved creating a docking grid with precise coordinates matching the native location of 6LU7 (inhibitor N3). The grid, sized 20 Å × 20 Å × 20 Å, was centered at coordinates -26.43° (X-axis), 12.58° (Y-axis), and 58.9° (Z-axis). Docking grids, incorporating these specifications, were generated using the "receptor grid generation" function within the Glide module in Schrödinger Maestro 12.8 [32]. Subsequently, the 'ligand docking' window of the Glide module in Schrödinger Maestro was populated with output files from the receptor grid generation, along with the ligands that had undergone minimization and preparation for docking. Settings included adjustable ligand sampling, an epic state penalty for the docking

DOI: https://doi.org/10.17509/ijost.v10i2.85146
p- ISSN 2528-1410 e- ISSN 2527-8045

score, and the standard precision protocol (SP) for docking precision [33]. To visualize only the best poses, the output was refined. These configurations were visualized in BIOVIA Discovery Studio, 2021 [34], depicting interacting complexes organized by assembly analysis.

2.4. Molecular Dynamics Study of the Best Docked Complex

A 100 nanoseconds Molecular Dynamics (MD) simulation was executed to validate the stability of the most favorably docked conformations of Tetrazole derivatives with the native ligand (inhibitor N3), as identified in the docking results. The primary aim was to comprehend the interaction dynamics and stability of the protein-ligand complex. Utilizing the system builder tool and the Desmond module from the Schrödinger 2021-2 suite, the MD simulation was conducted on a Linux operating system. The OPLS_2005 force field was applied, simulating the TIP3P (transferable intermolecular interaction potential 3 points) solvent model within an orthorhombic box measuring 10 Å × 10 Å × 10 Å. Counter ions were incorporated for model neutralization, and 0.15 M sodium chloride was introduced to replicate physiological conditions [50]. The Smooth Particle Mesh Ewald (PME) approach was employed at a temperature of 300 K and a pressure of 1.01325 bar throughout the simulation. The simulations adhered to isothermal-isobaric ensemble NPT (constant number of particles, pressure, and temperature) conditions. Specific equations were applied to compute the root-mean-square deviation (RMSD) and root-mean-square fluctuation (RMSF) trajectories, offering insights into the dynamics and stability of the protein-ligand interaction (see Equation (1) and (2).

$$\mathrm{RMSD_X} = \sqrt{\frac{1}{\mathrm{N}}\sum_{\mathrm{i=1}}^{\mathrm{N}}\left(\mathrm{r_i^t(t_x).}) - \mathrm{r_i(t_{ref})}\right)^2} \quad (1)$$

$$RMSF_i = \sqrt{\frac{1}{T}\sum_{t=1}^{T}\langle\left(r_i^t(t).) - r_i(t_{ref})\right)^2\rangle} \quad (2)$$

After the simulation, graphical representations, including plots and figures illustrating the interaction profiles between the ligands and proteins, along with visualizations of Root Mean Square Deviation (RMSD), Root Mean Square Fluctuation (RMSF), and the count of hydrogen bonds, were created using the Simulation Interaction Diagram wizard.

3. RESULTS AND DISCUSSION

3.1. Bibliometric Analysis of Research Trends

To evaluate the current research trends related to computational drug design targeting SARS-CoV-2 using pharmacokinetics, docking, and molecular dynamics, a bibliometric analysis was conducted using the keywords "pharmacokinetics AND docking AND molecular dynamics AND COVID" (see **Figure 3**). The search identified a total of more than four hundred scientific publications indexed from the year 2020 to 2025. Detailed information regarding the use of bibliometric is explained elsewhere [51-53].

The annual distribution of publications shows a distinct growth pattern that reflects the global research response to the COVID-19 pandemic. The number of studies was very limited in the early stage of the pandemic, but rapidly increased in the subsequent years, peaking in 2022 as research on COVID-19 therapeutics became highly active. After reaching its highest

DOI: https://doi.org/10.17509/ijost.v10i2.85146
p- ISSN 2528-1410 e- ISSN 2527-8045

point, the number of publications began to gradually decline in 2023, with decreasing publication activity observed in 2024 and 2025.

This decline does not reflect a reduction in the scientific value of this research domain. Instead, it suggests that much of the fundamental exploration during the critical phase of the pandemic has been accomplished, while the field is transitioning towards more specialized applications, clinical validations, and integration with broader therapeutic developments. Despite the downward trend, the sustained publication output indicates that computational drug discovery for COVID-19 remains a highly relevant area, especially for guiding drug repurposing, designing new inhibitors, and preparing for potential future viral outbreaks. The continuing exploration of molecular docking, pharmacokinetics modeling, and molecular dynamics simulation remains essential in supporting efficient, low-cost, and rapid drug design pipelines within the pharmaceutical engineering field.

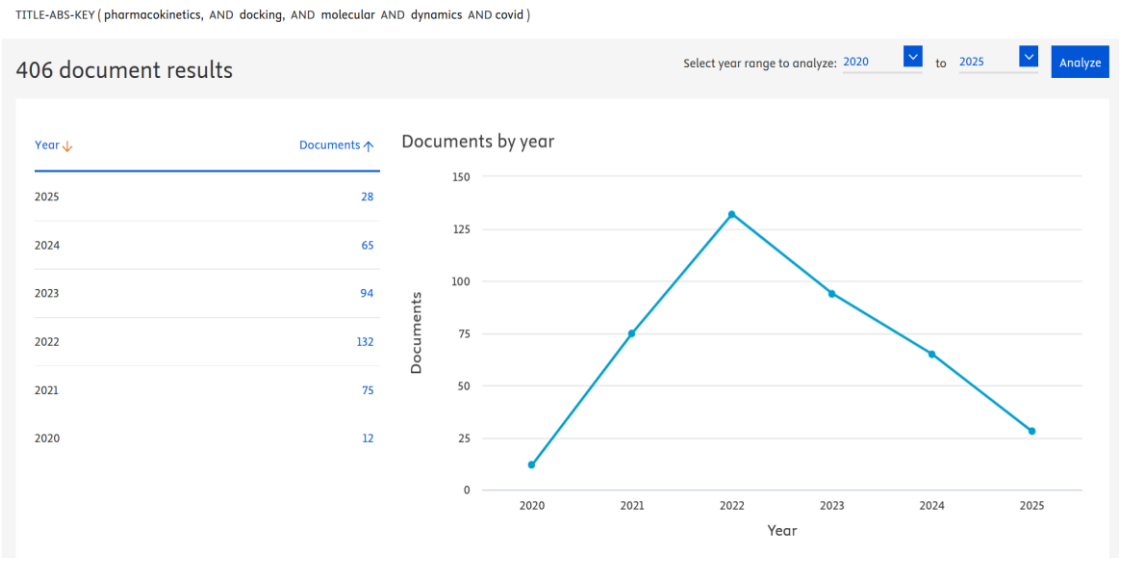

Figure 3. Annual distribution of publications related to pharmacokinetics, molecular docking, molecular dynamics, and COVID-19 from 2020 to 2025, based on bibliometric analysis. The data reflects research trends in computational drug discovery targeting SARS-CoV-2.

3.2. In Silico Prediction of Pharmacokinetic ADME Parameters

3.2.1. Analysis of Structure-Pharmacokinetic Properties Relationships of Studied Compounds Using SwissADME (SPR)

The radar plots generated by SwissADME (**Figure 4**) illustrate the predicted pharmacokinetic profiles of the studied compounds (3a-c, 4a-c) compared to the reference inhibitor N3. Compounds 3a, 3b, and 3c are characterized by a central scaffold linking two dimalononitrile-type units via various oxygenated alkyl chains (propane for 3a, butane for 3b, and hexane for 3c). The progressive elongation of the alkyl chain directly influences flexibility (FLEX), significantly increasing with chain length, as clearly indicated by the radar plots. Concurrently, this elongation slightly enhances lipophilicity (LIPO), thereby modestly reducing aqueous solubility (INSOLU). Additionally, a gradual and consistent decrease in unsaturation (INSATU) from compound 3a to 3c occurs due to the increasing saturation of the alkyl chains, diminishing the contribution of conjugated double bonds and unsaturated functional groups. Compounds 4a, 4b, and 4c, bearing highly polar tetrazol-1-ide groups, demonstrate notable increases in polarity (POLAR) and improved aqueous solubility compared to the 3-series

DOI: https://doi.org/10.17509/ijost.v10i2.85146
p- ISSN 2528-1410 e- ISSN 2527-8045

compounds. Similar to the previous series, flexibility rises with the elongation of the alkyl chain (propane for 4a, butane for 4b, and hexane for 4c). Again, a marked reduction in unsaturation (INSATU) is observed progressively from 4a to 4c, attributed to the extended alkyl chains becoming increasingly saturated, thus proportionally reducing the influence of unsaturated segments. The reference molecule N3, characterized by a complex peptide structure enriched with functional groups, exhibits a distinctive radar profile with notably high flexibility and lipophilicity, optimized for interaction with enzymatic targets such as the SARS-CoV-2 main protease. The substantial molecular size and structural complexity of N3 negatively influence its solubility and potentially limit oral bioavailability, contrasting with the studied compounds (3a-4c), which present more balanced pharmacokinetic properties favorable for oral administration. This detailed analysis clearly demonstrates the critical influence of alkyl chain length and saturation level on the predicted pharmacokinetic properties, establishing a robust structure-property relationship (SPR) within the framework of this SwissADME-based study.

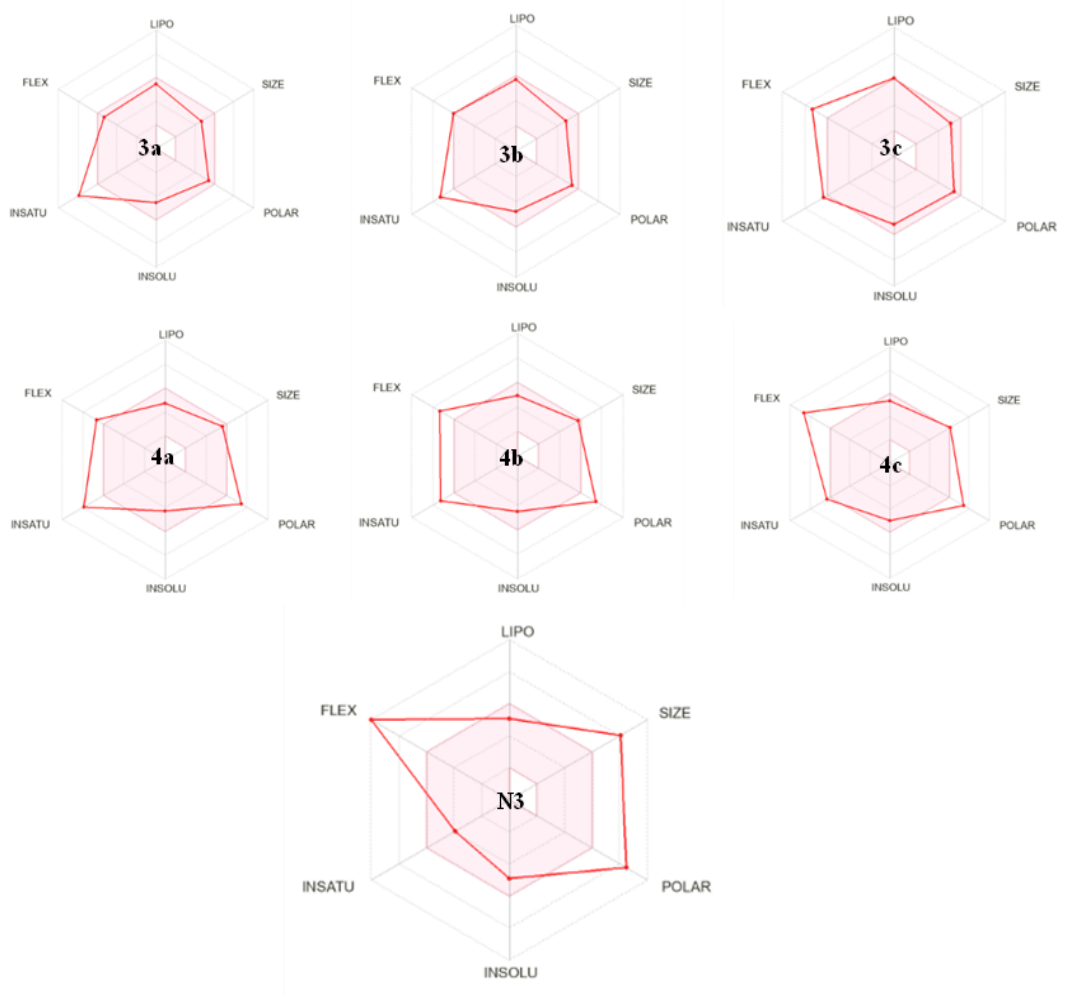

Figure 4. SwissADME radar plots of compounds 3a-c, 4a-c, and reference inhibitor N3.

3.2.2. In Silico Prediction of Pharmacokinetic ADMET Parameters

The investigation encompassed a comprehensive examination of the pharmacokinetics, ADMET features, and adherence to Lipinski's Rule of Five for all compounds, employing the QikProp application within the Schrödinger software [54]. The selected lead compounds exhibited robust pharmacokinetic characteristics and maintained compliance with Lipinski's

DOI: https://doi.org/10.17509/ijost.v10i2.85146
p- ISSN 2528-1410 e- ISSN 2527-8045

Rule of Five, underscoring their potential as drug candidates. Key parameters, including drug-likeness, dipole moment, molecular weight, hydrogen bond donor and acceptor traits, solvent accessible surface area, octanol/water coefficient, water-solubility, the number of probable metabolic reactions, and the coefficient of brain/blood barrier, were evaluated. Toxicity properties of compounds with favorable ADMET characteristics were scrutinized to assess potential adverse effects on humans. The chosen lead compounds demonstrated negligible or minimal toxicity after rigorous toxicity testing (**Table 1**). The test metabolites employed in this study are anticipated to possess significant solubility and intestinal permeability, facilitating their absorption into the bloodstream or through the intestinal wall for subsequent action. Crucially, the compounds exhibited no risk of hERG inhibition, mitigating the potential prolongation of the QT interval, a vital electrocardiographic parameter associated with cardiac contraction. In comparison to inhibitor N3, all compounds demonstrated favorable Lipinski Rule of Five values and predicted pharmacokinetic parameters without any violations, showcasing drug-like characteristics as potential infection inhibitors against SARS-CoV-2. This study advocates for the further exploration of these potential in vitro compounds in preclinical evaluations, emphasizing their promise as candidates for drug development.

Table 1. In Silico Lipinski's Rule of Five and Predicted ADMET Analysis for malonates 3a-3c, derivatives tetrazoles 4a-4c and the Native Ligand N3.

Ligands	(3a)	(3b)	(3c)	(4a)	(4b)	(4c)	N3
Molecular Weight	380.4	393.4	422.4	346.6	480	508.5	680.8
Donor HB	0	0	0	0	0	0	0
Acceptor HB	7.5	7.5	7.5	10.5	10.5	10.5	13.75
QPlogPo/w	2.66	3.06	3.86	1.61	1.98	2.69	2.34
Rule of five	0	0	0	1	1	2	2
SASA	770.4	801.9	867.7	841	869.7	936.8	1029.4
FOSA	147.3	181.8	247.4	142.9	176.7	238.0	637.3
FISA	267.3	267.4	267.3	379.5	377.8	379.5	215.5
PISA	355.6	352.7	352.9	316.3	315.2	319.1	176.7
Volume	1296.6	1358.5	1479.4	1456.2	1516.0	1633.4	2050.4
QPPCaco	28.8	28.8	28.8	2.4	2.5	2.4	2.58
QPlogBB	-3.4	-4.5	5.0	-4.5	-3.8	-5.3	-2.9
QPlogHERG	-7.3	-7.4	-7.6	-7.2	-7.3	-7.6	-0.7

SASA= Total solvent accessible surface area. Range 300.0 - 1000.0
FOSA= Hydrophobic component of the SASA. Range 0.0 - 750.0
FISA=Hydrophilic component of the SASA. Range 7.0 - 330.0
PISA= π (carbon and attached hydrogen) component of the SASA. Range 0.0 - 450.0
Volume: Total solvent-accessible volume in cubic angstroms. Range 500.0 - 2000.0
QPPCaco=Predicted apparent Caco-2 cell permeability. Range 25 -500
QPlogBB= Predicted brain/blood partition coefficient. Range -3.0 - 1.2
QPlogHERG= Predicted IC50 value for blockage of HERG K+ channel. concern below -5
RuleOfFive Number of violations of Lipinski's rule of five. The rules are: mol_MW < 500, QPlogPo/w < 5, donorHB ≤ 5, accptHB ≤ 10

3.2.3. pkCSM-based ADMET Evaluation of Compounds 3a-c, 4a-c and N3

The results obtained from PKCSM presented in **Table 2** offer a detailed analysis of key pharmacokinetic and toxicity parameters, establishing clear Structure-Property Relationships

DOI: https://doi.org/10.17509/ijost.v10i2.85146
p- ISSN 2528-1410 e- ISSN 2527-8045

(SPR) for the studied compounds (3a-c, 4a-c) compared to the reference inhibitor N3. Compounds 3a, 3b, and 3c display high percentages of predicted intestinal absorption (92.341%, 98.258%, and 96.85%, respectively), indicative of strong potential for effective oral bioavailability. This enhanced intestinal absorption correlates directly with their structural characteristics, particularly their optimized lipophilic-hydrophilic balance achieved through the introduction of moderately long oxygenated alkyl chains. Furthermore, none of these compounds inhibit CYP2D6, significantly reducing potential drug-drug interaction risks. However, they exhibit inhibition toward CYP3A4, an enzyme critical for drug metabolism, indicating a possibility of metabolic interactions that should be carefully evaluated during drug development. Notably, the Renal OCT2 substrate values are moderate (around 0.5), which suggests a lower potential for renal accumulation, thereby minimizing nephrotoxicity risks. In contrast, compounds 4a, 4b, and 4c show slightly lower intestinal absorption percentages (77.57%, 83.486%, and 82.078%), likely due to their increased polarity derived from tetrazol-1-ide functional groups. Despite lower absorption, this polarity provides improved aqueous solubility, facilitating formulation for oral administration. These compounds also avoid CYP2D6 inhibition but inhibit CYP3A4 similarly to compounds 3a-c. Importantly, their extremely low values for Renal OCT2 substrate (around 0.01 to 0.064) suggest negligible renal accumulation potential, underscoring their enhanced safety profiles. Evaluating cardiac toxicity, the QPlogHERG values obtained show notably low risks for the studied compounds (ranging from -7.2 to -7.6), indicating minimal likelihood of hERG channel inhibition and thus significantly reducing the potential for adverse cardiac effects, such as QT interval prolongation. Conversely, the reference inhibitor N3 has a notably higher QPlogHERG value (-0.7), suggesting an increased risk for hERG inhibition and potential cardiotoxicity. Consequently, correlating these pharmacokinetic outcomes with the previously assessed toxicity results clearly demonstrates that the studied compounds (3a-c, 4a-c) possess significantly improved safety profiles compared to N3. Their minimal predicted toxicity, favorable pharmacokinetic properties including high intestinal absorption and low renal accumulation and notably lower cardiac toxicity risk collectively reinforce their promising characteristics as oral therapeutic candidates.

Table 2. Predicted pharmacokinetic and toxicity parameters of studied compounds (3a-c, 4a-c) and Reference Inhibitor N3 using pkCSM.

Ligands	(3a)	(3b)	(3c)	(4a)	(4b)	(4c)	N3
Intestinal absorption (human) %	92,341	98,258	96,85	77,57	83,486	82,078	60,867
CYP2D6 inhibitor	No	No	No	No	No	No	No
CYP3A4 inhibitor	Yes	Yes	Yes	Yes	Yes	Yes	Yes
Renal OCT2 substrate	0,574	0,52	0,562	0,064	0,01	0,053	0,668
Total Clearance	No	No	No	No	No	No	No

3.2.4. Structural Influence on Melting, Boiling Points, and Plasma Half-lives (ADMETlab 3)

Drawing upon the ADMETlab 3 data presented in **Figure 5**, a targeted analysis was conducted to evaluate the melting points (°C), boiling points (°C), and plasma half-lives (h) of compound 3a-c and 4a-c, in comparison with the reference inhibitor N3 Compounds (3a-3c) exhibit melting points of 122.4 °C, 112.7 °C, and 116 °C, respectively, placing them in an intermediate range that implies adequate solid-state robustness and feasible pharmaceutical formulation. The variations in these values largely derive from the differences in alkyl chain length (propane, butane, hexane) and corresponding chain flexibility; in particular, the more

DOI: https://doi.org/10.17509/ijost.v10i2.85146
p- ISSN 2528-1410 e- ISSN 2527-8045

extended hexane chain lowers the melting point of 3c slightly due to reduced lattice packing. Meanwhile, the boiling points rise from 366.5 °C to 400 °C in step with longer chains, consistent with intensified Van der Waals interactions. Plasma half-lives (0.736-0.9 h) also increase, indicating that elevated lipophilicity and incremental structural stiffness help sustain these molecules in the bloodstream. Shifting to the 4-series, which contains tetrazol-1-ide groups, the melting points are substantially higher (201.8 °C, 189 °C, 185 °C). This reflects potent polar forces and the likelihood of hydrogen bonding, enhancing the crystal lattice. Similar to the 3-series, elongating the alkyl chain causes a minor drop in melting point, linked to decreased packing efficiency. Boiling points (306.4 °C, 303 °C, 314 °C) show more modest changes, as the interplay between polarity and molecular size evens out. Plasma half-lives (0.912, 0.9, 1 h) in this series exceed those of the 3-series, probably owing to the higher polarity restraining metabolic breakdown.

Regarding the reference inhibitor N3, it has a moderate melting point (122 °C), reminiscent of 3a, implying a balance among molecular flexibility, polar interaction potential, and packing capability. Its boiling point (298 °C) is relatively low compared to the other compounds, suggesting a partially peptide-like structure that does not foster the robust intermolecular contacts typical of elongated alkyl chains. N3's plasma half-life (0.86 h) is in line with those observed for the other substances, indicating a well-managed relationship between structural intricacy and polarity. Collectively, these findings highlight the pivotal role of alkyl chain length and functional polarity in modulating melting points, boiling points, and plasma half-lives. They reinforce dependable structure-property correlations (SPRs), forming a basis for future optimization of therapeutic entities.

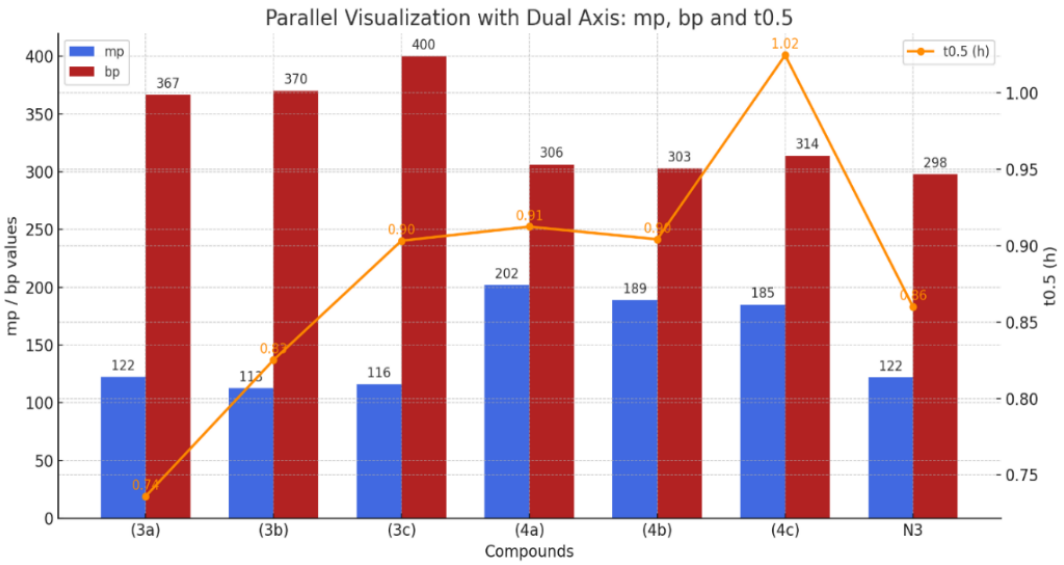

Figure 5. Melting points, boiling points, and half-lives of compounds 3a-c, 4a-c, and N3.

3.3. Molecular Docking Studies

A protein can engage with a ligand within an orthosteric pocket, influenced by factors such as size, structure, functional groups, and interactions. Molecular docking assesses the feasibility and compatibility of interactions between a protein (host) and a ligand (guest) in a complex [55]. The molecular docking analysis of the investigated compounds on SARS-CoV-2 Mpro revealed the highest binding affinity with malonates 3a-3c, as presented in Table 2, the binding affinities of -7.815 kcal/mol, -8.220 kcal/mol, and -8.093 kcal/mol were observed with malonates 3a, 3b, and 3c, respectively. Conversely, the molecular docking of ligand

DOI: https://doi.org/10.17509/ijost.v10i2.85146
p- ISSN 2528-1410 e- ISSN 2527-8045

derivatives tetrazoles 4a, 4b, and 4c with the SARS- CoV-2 Mpro protein demonstrated significant binding affinities of -6.838 kcal/mol, -6.120 kcal/mol, and -5.604 kcal/mol, respectively. The majority of ligands exhibited higher binding affinities than the Native Ligand (N3), indicating superior binding with the receptor protein. Multiple interactions, including hydrogen bonds, carbon-hydrogen bonds, alkyl interactions, Pi-alkyl interactions, Pi-sulfur interactions, alkyl interactions, Pi-donor hydrogen bonds, and van der Waals forces, were identified between the ligands and SARS-CoV-2 Mpro, as illustrated in **Figure 6** and detailed in **Table 3**. While the molecular docking results show promise, it is imperative to conduct further research, including clinical trials involving human subjects. These trials are essential to thoroughly evaluate the therapeutic efficacy, safety, and pharmacokinetics of the identified compounds.

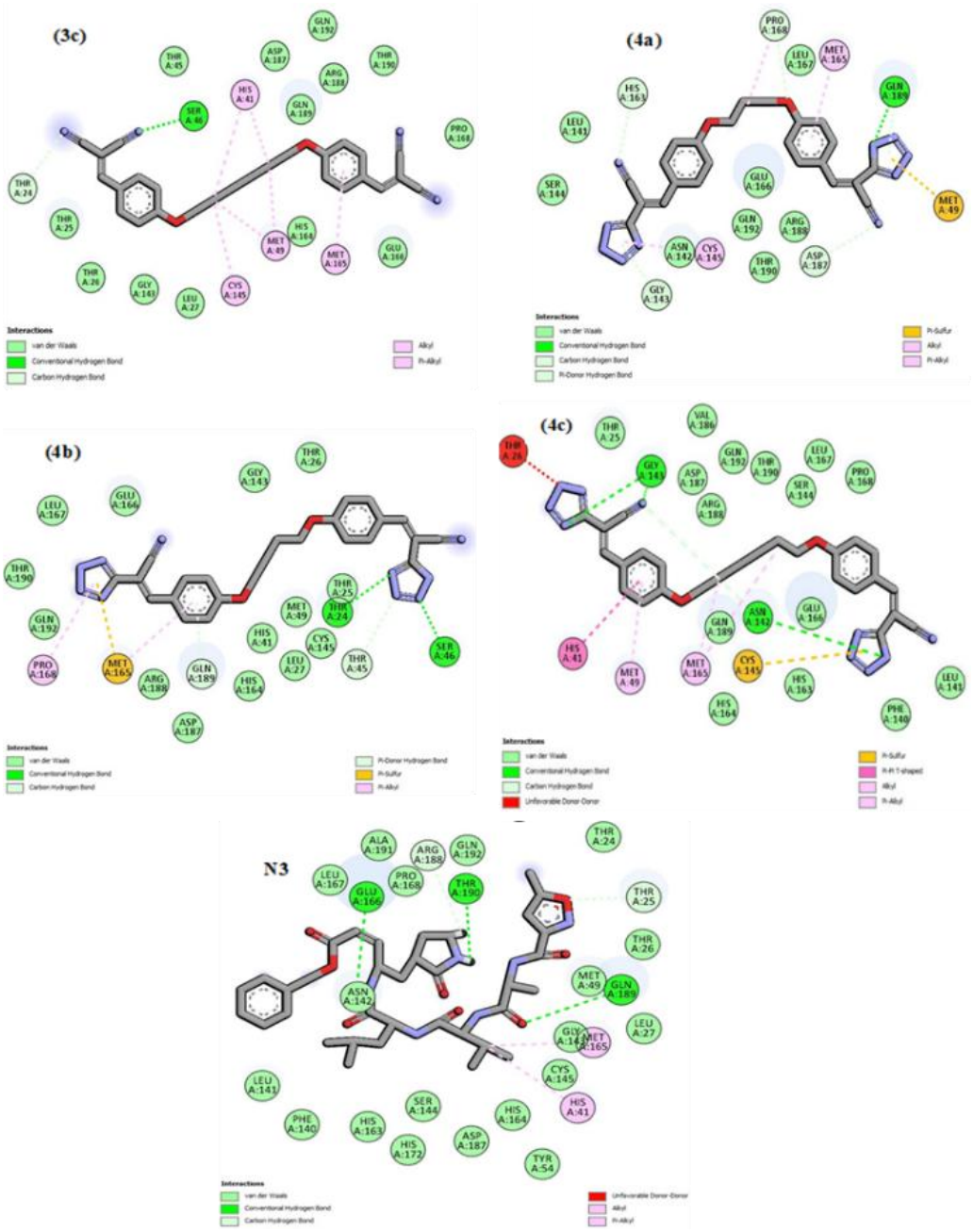

Figure 6. Intermolecular interactions between (3a) with SARS-CoV-2 Mpro, (3b) with SARSCoV-2 Mpro, (3c) with SARS-CoV-2 Mpro, (4a) with SARS-CoV-2 Mpro, (4b) with SARS-CoV-2 Mpro, (4c) with SARS-CoV-2 Mpro, (N3) with SARS-CoV-2 Mpro.

DOI: https://doi.org/10.17509/ijost.v10i2.85146
p- ISSN 2528-1410 e- ISSN 2527-8045

Table 3. The binding affinities and detailed interaction studies of malonates 3a-3c, derivatives tetrazoles 4a-4c and the Native Ligand N3 with SARS-CoV-2 Mpro.

Ligands	Dock Score (Kcal/mol)	Contributing Binding Residues	H-bonds
(3a)	-7.815	MET165-GLN189-MET49-CYS145-HIS41-SER46-THR45	2
(3b)	-8.220	SER46-THR45-MET49-CYS145-HIS41-MET165-GLN192	3
(3c)	-8.093	THR24-SER46-HIS41-CYS145-MET46-MET165	1
(4a)	-6.838	HIS163-PRO168-MET165-GLN189-MET49-ASP187-ASN142-GLY143	1
(4b)	-6.120	PRO168-MET165-THR24-SER46-THR45	2
(4c)	-5.604	GLY143-HIS41-MET49-MET165-CYS145-ASN142	3
N3	-7.750	GLU166-ASN142-THR190-GLN189-GLY143-HIS41	3

3.4. Molecular Dynamic Simulation

Molecular dynamics (MD) simulations serve as computational tools to examine the temporal movements and characteristics of atoms and molecules. These simulations employ principles of physics to calculate particle trajectories and interactions. By solving equations of motion, MD simulations provide valuable insights into dynamics and structural properties [23]. In our study, MD simulations were employed to assess the Root Mean Square Deviation (RMSD) of the C-alpha atoms for both the protein (depicted on the left Y-axis) and the ligand (depicted on the right Y-axis). Additionally, we analyzed the Root Mean Square Fluctuation (RMSF) and the protein-ligand contacts for the most favorable docking result involving malonate (3b) with the SARS-CoV-2 Mpro. **Figure 7(a)** presents the Root Mean Square Deviation (RMSD) scores plotted against time. The RMSD plot for the complex demonstrates stability from 10ns to 80ns. In the context of small proteins, deviations within the range of 0.5 - 3 Å are considered acceptable, while larger proteins may display a wider spectrum of RMSD values. This observation suggests that the protein maintains proper folding and exhibits an ideal ligand-receptor binding throughout the simulation. The RMSD of the ligand remains stable during most of the simulation. However, between 80ns and 100ns, there is a sudden increase in trajectory, indicating a change in the binding mode of the ligand. **Figure 7(b)** demonstrates the utility of Root Mean Square Fluctuation (RMSF) in identifying noteworthy fluctuations within the protein domain. In this complex, RMSF values varied between 0.6 and 2.4 Å, with the exception of the terminal amino acid residues. The N- and C-terminal tails of the protein exhibited greater fluctuations compared to other regions. Typically, secondary structure elements like alpha helices and beta strands exhibit higher rigidity than the unstructured regions of the protein, resulting in lesser fluctuation than the loop regions. The MD simulation results highlight the primary types of ligand-receptor interactions, specifically Hydrogen Bonds, Hydrophobic, Ionic, and Water Bridges. **Figure 7(c)**. In the SARS-CoV-2 Mpro complex with malonate (3b), certain residues, including THR25, SER46, GLN189, and GLN192, play pivotal roles in Hydrogen bond interactions. Moreover, PRO168 and MET165 contribute to robust hydrophobic interactions. These observations are consistent with predictions from molecular docking, indicating concordance between computational results and the preferred binding orientations and interactions of the ligand and receptor in this context. It's crucial to note that molecular docking and MD simulations are predictive tools and may not precisely

DOI: https://doi.org/10.17509/ijost.v10i2.85146
p- ISSN 2528-1410 e- ISSN 2527-8045

reflect real-world accuracy. Further validation through experimental studies is often necessary to confirm the results and gain a better understanding of the underlying mechanisms.

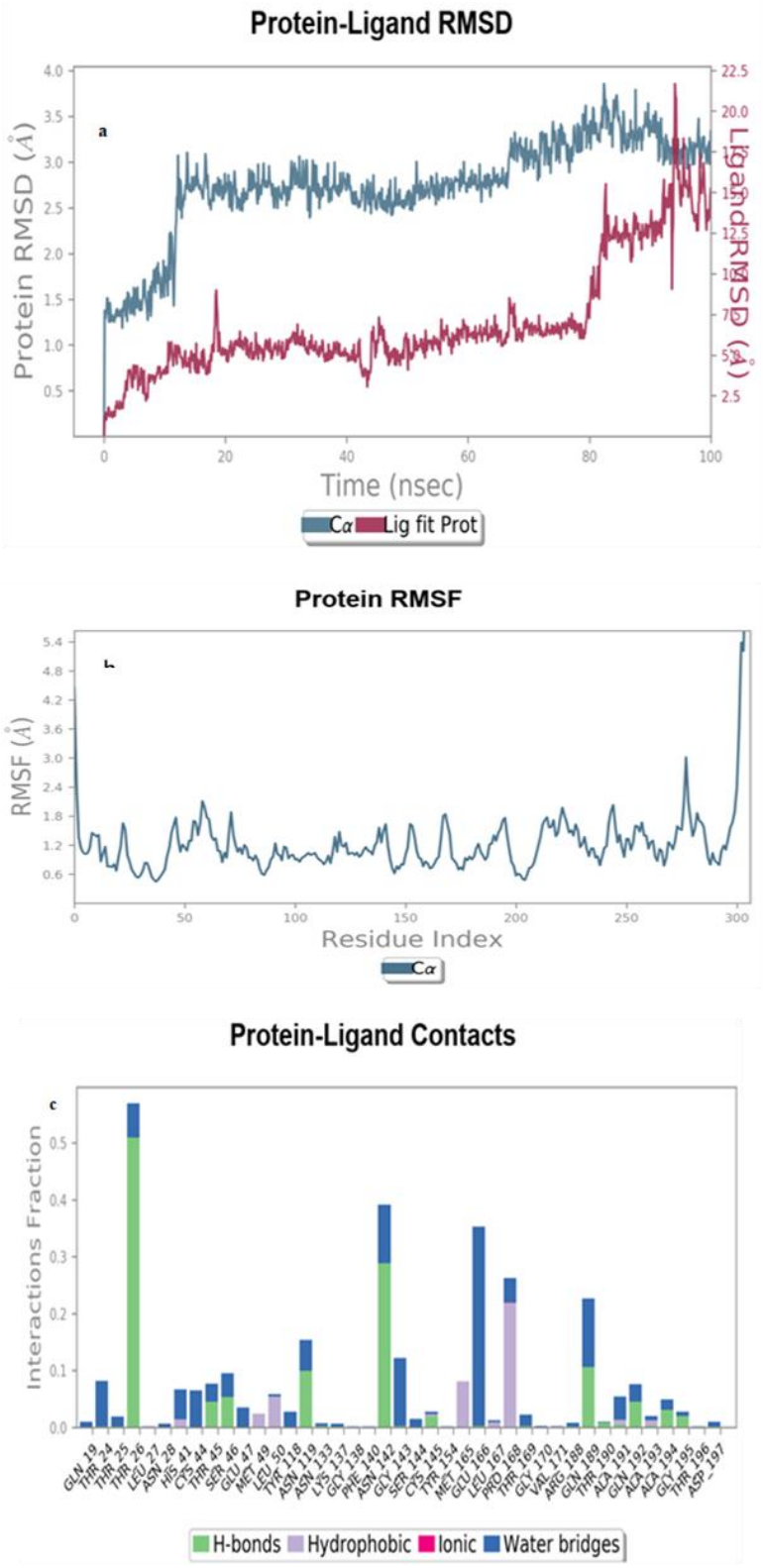

Figure 7. Investigating the Stability of the Docked Complex (**3b**) with SARS-CoV-2 Mpro through Molecular Dynamics Studies: Analysis of (a) Protein-Ligand RMSD, (b) Protein RMSF, and (c) Protein-Ligand Contacts.

DOI: https://doi.org/10.17509/ijost.v10i2.85146
p- ISSN 2528-1410 e- ISSN 2527-8045

3.5. Contribution to Sustainable Development Goals (SDGs)

The present study not only contributes to the advancement of antiviral drug discovery but also aligns directly with multiple SDGs set by the United Nations. The design and evaluation of novel malonate and tetrazole derivatives targeting SARS-CoV-2 Main Protease directly address SDG 3 (Good Health and Well-being), which emphasizes the importance of combating infectious diseases and improving global health outcomes. By applying computational engineering methods, this work contributes to accelerating drug discovery processes, thereby offering potential solutions to emerging health crises such as the COVID-19 pandemic.

In addition, the integration of advanced computational techniques such as molecular docking, pharmacokinetics prediction, and molecular dynamics simulation reflects the principles of SDG 9 (Industry, Innovation, and Infrastructure), which promotes scientific research, technological innovation, and infrastructure development. The application of in silico approaches allows for resource-efficient and time-effective evaluation of drug candidates, minimizing reliance on extensive laboratory testing in early research stages.

Furthermore, this research encourages international scientific collaboration and data sharing, supporting SDG 17 (Partnerships for the Goals). The interdisciplinary nature of the study highlights the value of collaborative efforts in addressing complex global challenges through integrated scientific methodologies.

Collectively, the outcomes of this research demonstrate how computational drug design can serve as a strategic tool not only for addressing immediate healthcare needs but also for contributing to long-term global sustainability and resilience within the broader SDG framework.

4. CONCLUSION

A thorough in-silico exploration of the malonate (3a–3c) and tetrazole (4a–4c) series found that malonate derivative 3b has a notably higher binding affinity for the SARS-CoV-2 Main Protease (Mpro, PDB ID: 6LU7) when compared with N3, the original ligand. The tested derivatives demonstrated beneficial pharmacokinetic attributes, minimal toxicity, and satisfactory drug-likeness on par with or superior to an established reference inhibitor. The encouraging computational insights from this research underline the promise of these compounds, especially 3b, for more advanced pharmacophore modeling and empirical evaluation. Ongoing in vitro and in vivo testing is warranted to confirm both therapeutic efficacy and safety, potentially leading to significant contributions in COVID-19 treatment strategies.

5. ACKNOWLEDGMENT

The authors would like to thank both Mohammed Premier University in Oujda, Morocco for using their lab.

6. AUTHORS' NOTE

The authors declare that there is no conflict of interest regarding the publication of this article. The authors confirmed that the paper was free of plagiarism.

DOI: https://doi.org/10.17509/ijost.v10i2.85146
p- ISSN 2528-1410 e- ISSN 2527-8045

7. REFERENCES

[1] Sharma, A., Tiwari, S., Deb, M. K., and Marty, J. L. (2020). Severe acute respiratory syndrome coronavirus-2 (SARS-CoV-2): A global pandemic and treatment strategies. *International Journal of Antimicrobial Agents,* 56(2), 106054.

[2] Muryanti, L., Fitria, L.N., Hanaya, G., and Triawan, F. (2021). Foldable bed design concept for covid-19 patient: A machine design case study. *ASEAN Journal of Science and Engineering*, *1*(2), 113-126.

[3] Pingak, C.T.R., Octaviani, M.A., Yuenan, G.C., and Triawan, F. (2022). Bed-stretcher for burial process of covid-19 corpse: A preliminary design and strength analysis. *ASEAN Journal of Science and Engineering*, *2*(1), 105-114.

[4] Chandra, C.E., and Abdullah, S. (2023). Jakarta COVID-19 forecast with bayesian PIRD multiwave model. *ASEAN Journal of Science and Engineering*, *3*(3), 227-242.

[5] Al Husaeni, D.N. (2022). Bibliometric analysis of briquette research trends during the covid-19 pandemic. *ASEAN Journal for Science and Engineering in Materials*, *1*(2), 99-106.

[6] Nasution, A.R., and Nandiyanto, A.B.D. (2021). Utilization of the google meet and quiziz applications in the assistance and strengthening process of online learning during the Covid-19 pandemic. *Indonesian Journal of Educational Research and Technology, 1*(2), 31-34.

[7] Ammatulloh, M.I., Permana, N., Firmansyah, R., Sa'adah, L.N., Izzatunnisa, Z.I., and Muthaqin, D.I. (2022). Strengthening character education of students through civics caring apps based on m-learning during the covid-19 pandemic. *Indonesian Journal of Educational Research and Technology*, *2*(2), 87-96.

[8] Abubakar, B.D., Kayode, F.E., Abiodun, M.H., Samson, A.B., and Abdulrasaq, A. (2022). Social media efficacy on prevention and control of covid-19 pandemic in Ilorin South Local Government Area, Kwara state. *Indonesian Journal of Educational Research and Technology*, *2*(3), 195-204.

[9] Fahrannisa, A.L., Muktiarni, M., and Mupita, J. (2022). The use of short stories as learning media for character education for elementary school students during the Covid-19 pandemic. *Indonesian Journal of Multidiciplinary Research, 2*(2), 237-244.

[10] Azzahra, S., Maryanti, R., and Wulandary, V. (2022). Problems faced by elementary school students in the online learning process during the Covid-19 pandemic. *Indonesian Journal of Multidiciplinary Research, 2*(2), 245-256.

[11] Ardiana, A., Nandiyanto, Kurniawan, T., and Bilad, M.R. (2022). Implementation of sticky note learning media to increase reading interest in 5th-grade students towards lesson books in the pandemic of Covid 19. *Indonesian Journal of Multidiciplinary Research, 2*(2), 265-270.

DOI: https://doi.org/10.17509/ijost.v10i2.85146
p- ISSN 2528-1410 e- ISSN 2527-8045

[12] Babalola, E.O., Otunla, F.L., and Omolafe, E.V. (2023). Undergraduates' level of acceptance and utilization of moodle platform for learning during covid-19 pandemic. *Indonesian Journal of Multidiciplinary Research, 3*(1), 31-40.

[13] Pena, H.J.P.D., Galindez, G.C., Sanduyogan, S.A., Vicente, S.S., and Organia, E.G. (2023). Lived experiences of overseas filipino nurses in western and middle-eastern countries amidst the covid-19 pandemic. *Indonesian Journal of Multidiciplinary Research*, *3*(2), 319-330.

[14] Ariyanti, N.D.S., and Maryanti, R. (2021). Developing the creativity of elementary school students in Cimahi, Indonesia through online learning media during the covid-19 pandemic. *Indonesian Journal of Teaching in Science*, *2*(1), 7-16.

[15] Pandoy, L.K.L., Diaz, Z.O.M.H., Salem, K.J.G., Damaso, J.M., Cabaylo, R.M., and Abo, C.P. (2022). Science teachers' lived experiences and challenges during covid-19 pandemic. *Indonesian Journal of Teaching in Science*, *2*(2), 155-174.

[16] Saputra, H., Albar, C. N., and Soegoto, D. S. (2022). Bibliometric analysis of computational chemistry research and its correlation with covid-19 pandemic. *Moroccan Journal of Chemistry*, *10*(1), 37-49.

[17] Weiss, S. R., and Navas-Martin, S. (2005). Coronavirus pathogenesis and the emerging pathogen severe acute respiratory syndrome coronavirus. *Microbiology and Molecular Biology Reviews, 69*(4), 635-664.

[18] Mohanty, S. K., Satapathy, A., Naidu, M. M., Mukhopadhyay, S., Sharma, S., Barton, L. M., and Parwani, A. V. (2020). Severe acute respiratory syndrome coronavirus-2 (SARS-CoV-2) and coronavirus disease 19 (COVID-19)-anatomic pathology perspective on current knowledge. *Diagnostic Pathology, 15*, 1-17.

[19] Khan, M. T., Irfan, M., Ahsan, H., Ahmed, A., Kaushik, A. C., Khan, A. S., and Wei, D. Q. (2021). Structures of SARS-CoV-2 RNA-binding proteins and therapeutic targets. *Intervirology, 64*(2), 55-68.

[20] More-Adate, P., Lokhande, K. B., Swamy, K. V., Nagar, S., and Baheti, A. (2022). GC-MS profiling of Bauhinia variegata major phytoconstituents with computational identification of potential lead inhibitors of SARS-CoV-2 Mpro. *Computers in Biology and Medicine, 147*, 105679.

[21] Merzouki, M., Bourassi, L., Abidi, R., Bouammali, B., Sabbahi, R., and Challioui, A. (2024). Deciphering the SARS-CoV-2 delta variant: Antiviral compound efficacy by molecular Docking, ADMET, and Dynamics studies. *Moroccan Journal of Chemistry*, *12*(3), 1153-1171.

[22] Merzouki, M., Challioui, A., Bourassi, L., Abidi, R., Bouammli, B., and El Farh, L. (2023). In silico evaluation of antiviral activity of flavone derivatives and commercial drugs against SARS-CoV-2 main protease (3CLpro). *Moroccan Journal of Chemistry*, *11*(1), 129-143.

DOI: https://doi.org/10.17509/ijost.v10i2.85146
p- ISSN 2528-1410 e- ISSN 2527-8045

[23] Hammoudan, I., Chtita, S., Bakhouch, M., and Temsamani, D. R. (2022). QSAR study of a series of peptidomimetic derivatives towards MERS-CoV inhibitors. *Moroccan Journal of Chemistry*, *10*(3), 405-416.

[24] Kawsar, S. M. A., Ferdous, J., Hossain, M. K., Kumer, A., Akash, S., and Chakma, U. (2023). Molecular docking against SARS-CoV-2 variants, antiviral, dynamics and quantum chemical modeling of mannopyranoside derivatives. *Moroccan Journal of Chemistry*, *11*(04), 1266-1286.

[25] Veerasamy, R., Seenivasa, R., Thangavelu, P., Rajak, H., and Pavadai, P. (2025). In silico docking, drug-likeness and toxicity prediction studies of bioactive compounds of eurycoma longifolia as potential multi-targeted antiviral agents against SARS-CoV-2. *Moroccan Journal of Chemistry*, *13*(1), 381-404.

[26] Bourhou, C., Benouda, H., Bellaouchi, R., Merzouki, M., Fraj, E., Harit, T., and Bouammali, B. (2023). Synthesis of novel tetrazolic derivatives and evaluation of their antimicrobial activity. *Journal of Molecular Structure, 1278,* 134913.

[27] Fraj, E., Hassiba, M., Bouammali, H., Merzouki, M., Bourhou, C., Zughaier, S. M., and Bouammali, B. (2025). Design, Synthesis, and Anti-Inflammatory Evaluation In Vitro and In Silico of Novel Flavone Derivatives. *Chemistry Select, 10*(9), e202405663.

[28] Hasan, A. H., Hussen, N. H., Shakya, S., Jamalis, J., Pratama, M. R. F., Chander, S., and Murugesan, S. (2022). In silico discovery of multi-targeting inhibitors for the COVID-19 treatment by molecular docking, molecular dynamics simulation studies, and ADMET predictions. *Structural Chemistry, 33*(5), 1645-1665.

[29] Wihadi, M. N. K., Merzouki, M., Ma'arif, A. S., Grasianto, G., and Santosa, S. J. (2024). Insights of auric ion adsorption in the presence of ferric and hexavalent chromium species on Mg/Al layered double hydroxides. *Moroccan Journal of Chemistry, 12*(2), 854-869.

[30] Alshahateet, S. F., Altarawneh, R. M., Al-Tawarh, W. M., Al-Trawneh, S. A., Al-Taweel, S., Azzaoui, K., and Jodeh, S. (2024). Catalytic green synthesis of Tin (IV) oxide nanoparticles for phenolic compounds removal and molecular docking with EGFR tyrosine kinase. *Scientific Reports, 14*(1), 6519.

[31] Loukili, E. H., Merzouki, M., Taibi, M., Elbouzidi, A., Hammouti, B., Yadav, K. K., and Choi, J. R. (2024). Phytochemical, biological, and nutritional properties of the prickly pear, Opuntia dillenii: A review. *Saudi Pharmaceutical Journal, 32*(10), 102167.

[32] Bouakline, H., Bouknana, S., Merzouki, M., Ziani, I., Challioui, A., Bnouham, M., and El Bachiri, A. (2024). The phenolic content of pistacia lentiscus leaf extract and its antioxidant and antidiabetic properties. *The Scientific World Journal*, *2024*(1), 1998870.

[33] Boumezzourh, A., Ouknin, M., Merzouki, M., Dabbous-Wach, A., Hammouti, B., Umoren, P. S., and Majidi, L. (2023). Acetylcholinesterase, Tyrosinase, α-Glucosidase inhibition by Ammodaucus leucotrichus Coss. & Dur. Fruits Essential oil and ethanolic extract and molecular docking analysis. *Moroccan Journal of Chemistry*, *11*(04), 11-4.

DOI: https://doi.org/10.17509/ijost.v10i2.85146
p- ISSN 2528-1410 e- ISSN 2527-8045

[34] Mili, A., Das, S., Nandakumar, K., and Lobo, R. (2023). Molecular docking and dynamics guided approach to identify potential anti-inflammatory molecules as NRF_2 activator to protect against drug-induced liver injury (DILI): A computational study. *Journal of Biomolecular Structure and Dynamics*, *41*(19), 9193-9210.

[35] Kerans, G., Sanjaya, Y., Liliasari, L., Pamungkas, J., and Ate, G., Y. (2024). Effect of substrate and water on cultivation of Sumba seaworm (nyale) and experimental practicum design for improving critical and creative thinking skills of prospective science teacher in biology and supporting sustainable development goals (SDGs). *ASEAN Journal of Science and Engineering*, *4*(3), 383-404.

[36] Makinde, S.O., Ajani, Y.A., and Abdulrahman, M.R. (2024). Smart learning as transformative impact of technology: A paradigm for accomplishing sustainable development goals (SDGs) in education. *Indonesian Journal of Educational Research and Technology*, *4*(3), 213-224.

[37] Gemil, K.W., Na'ila, D.S., Ardila, N.Z., and Sarahah, Z.U. (2024). The relationship of vocational education skills in agribusiness processing agricultural products in achieving sustainable development goals (SDGs). *ASEAN Journal of Science and Engineering Education*, *4*(2), 181-192.

[38] Haq, M.R.I., Nurhaliza, D.V., Rahmat, L.N., and Ruchiat, R.N.A. (2024). The influence of environmentally friendly packaging on consumer interest in implementing zero waste in the food industry to meet sustainable development goals (SDGs) needs. *ASEAN Journal of Economic and Economic Education*, *3*(2), 111-116.

[39] Basnur, J., Putra, M.F.F., Jayusman, S.V.A., and Zulhilmi, Z. (2024). Sustainable packaging: Bioplastics as a low-carbon future step for the sustainable development goals (SDGs). *ASEAN Journal for Science and Engineering in Materials*, *3*(1), 51-58.

[40] Maulana, I., Asran, M.A., and Ash-Habi, R.M. (2023). Implementation of sustainable development goals (SDGs) no. 12: Responsible production and consumption by optimizing lemon commodities and community empowerment to reduce household waste. *ASEAN Journal of Community Service and Education*, *2*(2), 141-146.

[41] Nurnabila, A.T., Basnur, J., Rismayani, R., Ramadhani, S., and Zulhilmi, Z. (2023). Analysis of the application of mediterranean diet patterns on sustainability to support the achievement of sustainable development goals (SDGs): Zero hunger, good health and well beings, responsible consumption, and production. *ASEAN Journal of Agricultural and Food Engineering*, *2*(2), 105-112.

[42] Awalussillmi, I., Febriyana, K.R., Padilah, N., and Saadah, N.A. (2023). Efforts to improve sustainable development goals (SDGs) through education on diversification of food using infographic: Animal and vegetable protein. *ASEAN Journal of Agricultural and Food Engineering*, *2*(2), 113-120.

[43] Rahmah, F.A., Nurlaela, N., Anugrah, R., and Putri, Y.A.R. (2024). Safe food treatment technology: The key to realizing the sustainable development goals (SDGs) zero hunger and optimal health. *ASEAN Journal of Agricultural and Food Engineering*, *3*(1), 57-66.

DOI: https://doi.org/10.17509/ijost.v10i2.85146
p- ISSN 2528-1410 e- ISSN 2527-8045

[44] Keisyafa, A., Sunarya, D.N., Aghniya, S.M., and Maula, S.P. (2024). Analysis of student's awareness of sustainable diet in reducing carbon footprint to support sustainable development goals (SDGs) 2030. *ASEAN Journal of Agricultural and Food Engineering*, *3*(1), 67-74.

[45] Nandiyanto, A. B. D., Kaniawati, I., Kurniawan, T., Farobie, O., and Bilad, M. R. (2024). Chemical reaction mechanism from pyrolysis degradation of polystyrene styrofoam plastic microparticles based on FTIR and GC-MS completed with bibliometric literature review to support sustainable development goals (SDGs). *Moroccan Journal of Chemistry*, *12*(3), 1380-1398.

[46] Nandiyanto, A. B. D., Putri, N. R., Salimah, N. N., Al'Hafsah, S. H., Yunatraya, S. A., Fiandini, M., and Sukrawan, Y. (2025). Utilizing Cassava Peel-Derived Carbon Biochar for Ammonia Adsorption to Support Hydrogen Storage and Sustainable Development Goals (SDGs): Effect of Microparticle Size and Isothermal Analysis. *Moroccan Journal of Chemistry*, *13*(1), 424-439.

[47] Nandiyanto, A. B. D., Firdaus, N. N., Anzety, N. D., Fiandini, M., Farobie, O., Bilad, M. R., and Sukrawan, Y. (2025). Carbon Biochar Microparticles from Mango Peel as a Sustainable Adsorbent for Ammonia Storage in Supporting Hydrogen Energy Systems and Sustainable Development Goals (SDGs). *Moroccan Journal of Chemistry*, *13*(2), 531-548.

[48] Nandiyanto, A. B. D., Fitriani, A. F., Pradana, R. A., Ragadhita, R., Azzaoui, K., and Piantari, E. (2024). Green innovation in brake pad production: Harnessing teak powder and clam shells as sustainable alternatives for subtractive residual waste. *Moroccan Journal of Chemistry*, *12*(2), 714-733.

[49] Nandiyanto, A. B. D., Ragadhita, R., and Anggiat, L. S. (2024). Synthesis of barium oxide nanoparticles: Optical properties and application in degradation indigotine dye. *Moroccan Journal of Chemistry*, *12*(2), 627-642.

[50] Cordina, R. J., Smith, B., and Tuttle, T. (2023). COGITO: A coarse-grained force field for the simulation of macroscopic properties of triacylglycerides. *Journal of Chemical Theory and Computation*, *19*(4), 1333-1341.

[51] Rochman, S., Rustaman, N., Ramalis, T.R., Amri, K., Zukmadini, A.Y., Ismail, I., and Putra, A.H. (2024). How bibliometric analysis using VOSviewer based on artificial intelligence data (using ResearchRabbit Data) : Explore research trends in hydrology content. *ASEAN Journal of Science and Engineering*, *4*(2), 251-294.

[52] Al Husaeni, D.F., and Nandiyanto, A.B.D. (2022). Bibliometric using VOSviewer with publish or perish (using google scholar data) : From step-by-step processing for users to the practical examples in the analysis of digital learning articles in pre and post covid-19 pandemic. *ASEAN Journal of Science and Engineering*, *2*(1), 19-46.

[53] Al Husaeni, D.N., and Al Husaeni, D.F. (2022). How to calculate bibliometric using VOSviewer with Publish or Perish (using Scopus data): Science education keywords. *Indonesian Journal of Educational Research and Technology*, *2*(3), 247-274.

DOI: https://doi.org/10.17509/ijost.v10i2.85146
p- ISSN 2528-1410 e- ISSN 2527-8045

[54] Abbaoui, Z., Merzouki, M., Oualdi, I., Bitari, A., Oussaid, A., Challioui, A., and Diño, W. A. (2024). Alzheimer's disease: In silico study of rosemary diterpenes activities. *Current Research in Toxicology*, *6*, 100159.

[55] Bekkouch, A., Merzouki, M., El Mostafi, H., Elhessni, A., Challioui, A., Mesfioui, A., and Touzani, R. (2024). Potential inhibition of ALDH by argan oil compounds, computational approach by docking, ADMET and molecular dynamics. Moroccan *Journal of Chemistry*, *12*(2), 676-695.

DOI: https://doi.org/10.17509/ijost.v10i2.85146
p- ISSN 2528-1410 e- ISSN 2527-8045